BOLTED JOINT FRACTURE MODES IN GLASS-FIBRE REINFORCED POLYESTER

B. Vangrimde[1] and R. Boukhili[1]

[1] *Center for Applied Research on Polymers, École Polytechnique de Montréal, CP 6079, succursale Centre-Ville, Montréal, Quebec, H3C 3A7, Canada*

SUMMARY: The performance of bolted joints in composite materials can be optimized in many ways, including optimization of the joint geometry and optimization of the fibre orientation and stacking sequences. In this investigation, the performance of different material configurations is evaluated using the standard ASTM D5961 coupon geometry. The standard advises however the use of a quasi-isotropic lay-up for the bearing response test. Since other lamination sequences are used in this investigation, the preferred bearing failure is not guaranteed and other failure mechanisms are observed. Moreover, it is intended to show that in general purpose composite laminates, the performance of a bolted joint is a complex procedure that should be assessed by a careful examination of the whole mechanical response along with a clear description of the damage growth.

KEYWORDS: bolted joints, fastening, fracture modes, bearing, shearout, GRP.

INTRODUCTION

This paper presents the second part of a study dealing with the mechanical behaviour of single-bolt double shear joints in composite laminates. The first part [1] focused on the stress-strain response and this part focuses on the fracture mode and the strength. Studies on mechanical fastening of general purpose composite laminates consists mainly of studies on pultruded products, reviewed recently by Turvey [2]. Most of the research is done on one commercial pultruded product. Because a bolted joint reduces the strength of a structure by more than 50% for a single-row joint, the choice of the laminate to be used can depend on the bolted joint strength rather than on the unnotched strength or stiffness. Therefore, it has to be questioned if the right laminates are used.

Six different laminates with varying contents of 0°, 90° and mat reinforcements were tested in our laboratory to explore the bolted behaviour of different laminate lay-ups. The coupon geometry chosen was the one proposed by the ASTM D5961 standard test method for bearing response of polymer matrix composite laminates. The basic failure modes for shear-loaded bolted joints are presented in Fig. 1. Also defined in Fig. 1 are the width “w” and end distance “e” of the coupon. The end distance is the distance from the centre of the hole to the non-loaded end of the coupon. The hole diameter will be referred to as “D”. Net tension failure typically occurs for a small pitch distance ratio “w/D”. A small end distance ratio

"e/D" leads to shearout failures. Cleavage occurs for laminates with little transverse reinforcement. The bearing failure mode is non-catastrophic and is therefore preferred for design purposes. However, the bearing failure requires a sufficient width, a sufficient end distance and lamination sequences that are close to quasi-isotropy. Although the other failure modes are usually catastrophic, Abd-El-Naby and Hollaway [3] reported ductile shearout failures for pultruded sheets with a large end distance. Delamination by interlaminar shear between mat reinforcements and 0° rovings played an important role in the damage mechanisms reported by these authors.

EXPERIMENTAL PROCEDURES

Materials

The materials under investigation were compression molded from three different glass-fibre reinforced polyester prepregs. The compression molding process was chosen in order to make arbitrarily large plates and for the ease of varying lamination sequences. The first prepreg used contains unidirectional continuous rovings and mat (0°/mat), the second prepreg contains bi-directional rovings and mat (0°/90°/mat) and the third prepreg contains only mat (mat). These prepregs had approximate thicknesses of respectively 0.62 mm, 0.78 mm and 1.24 mm. From these three elementary prepregs, six laminates were molded according to the sequences shown in Table 1. Table 1 also shows the content of 0° rovings, 90° rovings and mat fibre reinforcements compared to the total fibre content. The fibre volume was approximately 40 % for all the laminates and nominal laminate thickness "h" was 6.2 mm. Care was taken during the lamination process to avoid 0° plies on the surface. In doing so, the outer plies can delay buckling of compressed 0° rovings. The thick (mat) ply was always kept around the midsection of the laminate. Some 0° plies are blocked together which could adversely affect bolted joint strength.

Table 1: Material configurations and experimental results.

	0^o (%)	90^o (%)	mat (%)	Material configuration	σ_x^u (MPa)	E_x (GPa)	σ_y^u (Mpa)
A	63	0	37	$[(mat/0^o)/(0^o/mat)_4]_s$	510	26.9	70
B	34	34	32	$[(mat/90^o/0^o)/(0^o/90^o/mat)_3]_s$	341	21.1	(341)
C	0	0	100	$[(mat)_5]$	210	15.9	(210)
D	38	0	62	$[(mat/0^o)/(0^o/mat)_2/mat]_s$	398	23.2	140
E	33	9	58	$[(mat/90^o/0^o)/(0^o/mat)_2/mat]_s$	349	21.3	187
F	56	9	35	$[(mat/90^o/0^o)/(0^o/mat)_4]_s$	441	-	-

Test method

Longitudinal and transverse tensile tests were performed according to the ASTM D3039 testing procedure in order to provide a reference point for comparing bolted joint strengths. For the longitudinal tests, an extensometer was used to determine the longitudinal modulus. Results in Table 1 indicate that the longitudinal tensile strength "σ_x^u" and modulus "E_x" are strongly dependent on the amount of 0° fibres. Laminates B and C were not tested transversely because they should be equally resistant in longitudinal and transverse directions. The other laminates show a strong reduction of the strength for the transverse direction.

To evaluate the bolted joint strength, a testing fixture was designed according to the specifications given by the ASTM D5961 standard. To allow a wide range of bolt diameters and coupon thicknesses, the design was not fully equivalent to the ASTM testing fixture. A drawing of the fixture used is shown in Fig. 2. The fixture was mounted on a MTS 810 servohydraulic fatigue testing machine and data was collected every 0.1 s by Teststar II software. Loading speed was 2 mm/min.

The bolt diameter was selected in function of the hole diameter over laminate thickness ratio "D/h". For a small ratio, the bolt bending is important while for a large ratio the instability effects in glass-fibre reinforced laminates reduce the strengths [4]. A hole diameter of 9.53 mm (D/h= 1.54) was chosen as a compromise between these two effects. A bolt of 9.23 mm and steel washers of outer diameter 22.6 mm, inner diameter 9.7 mm and a thickness of 2.5 mm were used. The bolts were tightened at 3Nm.

The coupons were machined with pitch distance ratio w/D=6 and end distance ratio e/D=3. This resulted in a nominal width "w" of 57 mm and edge distance "e" of 28.5 mm. Two LVDTs mounted on the loading plates monitored the bearing deformation at a distance "L" below the bolt hole center. At least 3 coupons were tested for each laminate in the longitudinal direction and for laminates A, D and E in the transverse direction.

RESULTS AND DISCUSSION

Presentation method

As suggested by the standard, the data is presented in the form of bearing stress (σ_{br})- bearing strain (ε_{br}) curves. The bearing stress is defined by Eqn 1 as the applied load "P" divided by the hole diameter and the thickness of the laminate. The bearing strain is defined by Eqn 2 as the average of the two LVDT displacements, "δ_a" and "δ_b", divided by the hole diameter.

$$\sigma_{br} = \frac{P}{D.h} \quad (1)$$

$$\varepsilon_{br} = \frac{\left(\delta_a + \delta_b\right)}{D} \quad (2)$$

The deformation caused by tensile strain in the coupon was subtracted from the measured LVDT displacements, as suggested by Vangrimde and Boukhili [1].

Bearing stress-bearing strain plots and failure modes

Typical σ_{br}-ε_{br} plots for laminates A, B and C are shown in Fig. 3. Fig. 4 shows plots for laminates D, E and F. Both are for longitudinal tests. The stress-strain behaviour of the different laminates is very similar until a bearing strain of 0.06 where a first damage mechanism occurs. This damage is confined under the washers. Since mat plies are present in all the laminates and the phenomenon is observed in all laminates, this first damage sign can probably be attributed to a damage mechanism in the mat reinforcements. Since the bearing stiffnesses of the laminates are close to one another, this corresponds to a bearing stress between 400 MPa and 480 MPa for the laminates under consideration.

The laminates with the highest amount of 0° fibres, A and F, fail catastrophically at this point. Fig. 5 clearly shows the involved shearout failures. The material in front of the bolt was pushed out of the laminate, except for the surface mat layer in laminate A and the surface mat and 90° layers in laminate F.

In order to examine the progress of the failure in the inner plies, a resin burn-off was performed on the tested specimens. Peeling of the different plies shows quite clearly the

deformation and damage experienced by the inner plies. For laminate A it showed that the mat was sheared along the shear planes. The 0° rovings were also sheared along the shear planes, but the fibres in the rovings looked intact. For material F, the resin burnoff showed that the 90° rovings close to the bolt hole acted as "beams" resisting the push out of the material in front of the bolt.

The other laminates pick up load again after the first failure sign albeit with a reduced stiffness. It should be mentioned that this first failure sign satisfies the damage load definition by Cooper and Turvey [5].

Laminate C failed in net tension, as expected because of its low longitudinal tensile strength compared to relatively high shear and transverse tensile strengths. The bearing stress first begins to diminish, while the tension crack develops and then drops suddenly as the crack develops through the full width of the laminate.

In laminate D, some of the (0°/mat) prepregs of laminate A were replaced by (mat) prepregs. Laminate D can be looked upon as an interpolation between laminates A and C. The mat provides relatively high shear and transverse strength while the remaining 0° rovings assure a fairly high longitudinal tensile strength. As seen on Fig. 4 the load does not drop totally after the ultimate bearing strength "F_{bru}" has been reached, contrary to the laminates A and C. Fig. 5 shows how the outer (mat/0°)/(0°/mat) plies have delaminated from the inner mat plies. These delaminations cause the sudden load drop on Fig. 4. Then, the load is carried further by the inner mat plies. These are crushed ahead of the bolt by bearing, as shown by resin burn-off.

Laminate B consisting of nearly equal amounts of 0° rovings, 90° rovings and mat was thought to be a good choice because the presence of 90° fibres is known to be beneficiary to the bolted joint strength. Fig. 3 shows that the laminate does not fail at the low strains of laminates A or C that do not have 90° fibres but nevertheless, the failure stays catastrophic. Inspection of the failure in Fig. 5 shows that the final failure mode is shearout and that more damage mechanisms have been involved than in the former laminates. Burn-off of the resin showed that the area close to the bolt was crushed, which indicates the beginning of bearing failure. The end distance was too short however for the bearing failure to fully develop and catastrophic failure was caused by shearout.

Finally laminate E, which resembles laminate D but with some of the 0° rovings and mat replaced by 90° rovings, has a failure mode much resembling that of laminate D: outer plies have delaminated despite of the 90° rovings which try to keep the laminate together. Like laminate D, once the delamination took place, the load was taken by the inner mat plies and the load drop was not total. An extensive crushed zone in these inner mat plies, indicates the bearing mechanism that develops in these plies.

Transverse failures of laminates A, D and E were all tension mode failures. For laminate E, it was observed that the outer (mat/90°) plies, which become (mat/0°) plies in the transverse direction, delaminated from the rest of the material at one side of the hole after which the inner plies failed in tension.

Strength

Longitudinal and transverse tensile strengths are reported in Table 2 as are the 90% confidence levels. The large confidence levels are caused by the small number of tests, rather than by the scattering in the results. Strength values of laminates B, C, D and E in longitudinal tests are high and close to one another. Laminate A is clearly the weakest, followed by laminate F. The transverse tests indicate that the efficiency is higher in this direction: the ratio bolted joint strength over unnotched strength is substantially higher than for the longitudinal tests. The high mat content in laminate D and the 90° and mat reinforcements in laminate E provide a good transverse strength. Laminates B and C, which did not need to be tested transversally, are the most resistant in the transverse direction.

Table 2: Longitudinal and transverse bearing strength.

	$F_{bru,\ longitudinal}$ (MPa)	90% conf. level (MPa-MPa)	$F_{bru,\ transversal}$ (MPa)	90 % conf. level (MPa-MPa)
A	414	[403-425]	240	[234-246]
B	525	[513-537]	(525)	(513-537)
C	504	[454-554]	(504)	(454-554)
D	501	[441-561]	378	[369-387]
E	511	[480-542]	455	[412-498]
F	428	[390-466]	-	-

CONCLUSION

Bolted joint tests according to ASTM standard D5961 have been conducted on six glass-fibre reinforced polyester laminates with different 0° roving, 90° roving and mat contents. The bearing-stress bearing-strain plots showed that close to a 0.06 bearing strain, damage developed in all laminates. Laminates with a high amount of 0° rovings (laminates A and F) failed at this point in shearout. In contrast, laminates with a sufficient amount of off-axis fibres can accommodate the first damage and support higher bearing strains, albeit with a reduced stiffness. Absence of 0° rovings in the mat laminate (C) causes its tension failure. A lay-up with nearly equal amounts of 0°, 90° and mat reinforcement (laminate B) showed the beginning of a ductile bearing failure but the end distance was not adequate to allow full development of this mechanism. Laminates with a relatively high amount of mat (D and E), showed a double failure mechanism: first the outer 0° plies delaminate from the inner mat plies, then the reduced load is reacted by a bearing failure mechanism in the mat plies.

Strength of the more orthotropic laminates (A and F) was poor compared to the strength of the more quasi-isotropic ones. Nearly equal bolt bearing strengths developed for the more quasi-isotropic laminates. These laminates also have superior failure strains, which can be useful for the design of multiple row joints.

ACKNOWLEDGEMENTS

The authors wish to acknowledge the support given by the Natural Sciences and Engineering Research Council of Canada (NSERC) and the Québec FCAR Fund (Formation de Chercheurs et Aide à la Recherche).

REFERENCES

1. Vangrimde, B. and Boukhili, R., "Measuring Bolted Joint Bearing Deformation and Stiffness", *Proceedings of the Twelfth International Conference on Composite Materials*, Paris, France, July 5-9, 1999.

2. Turvey, G.J., "Single-bolt Tension Joint Tests on Pultruded GRP Plate - Effects of Tension Direction Relative to Pultrusion Direction", *Composite Structures*, Vol. 42, 1998, pp. 341-351.

3. Abd-El-Naby, S.F.M. and Hollaway, L., "The Experimental Behaviour of Bolted Joints in Pultruded Glass/Polyester Material. Part 1: Single-bolt Joints" *Composites*, Vol. 24, No. 7, 1993, pp. 531-538.

4. Kretsis, G. and Matthews, F.L., "The strength of bolted joints in glass fibre/epoxy laminates", *Composites*, Vol. 16, 1985, pp. 92-102.

5. Cooper, C. and Turvey, G.J., "Effects of Joint Geometry and Bolt Torque on the Structural Performance of Single Bolt Tension Joints in Pultruded GRP Sheet Material", *Composite Structures*, Vol. 32, 1995, pp. 217-226.

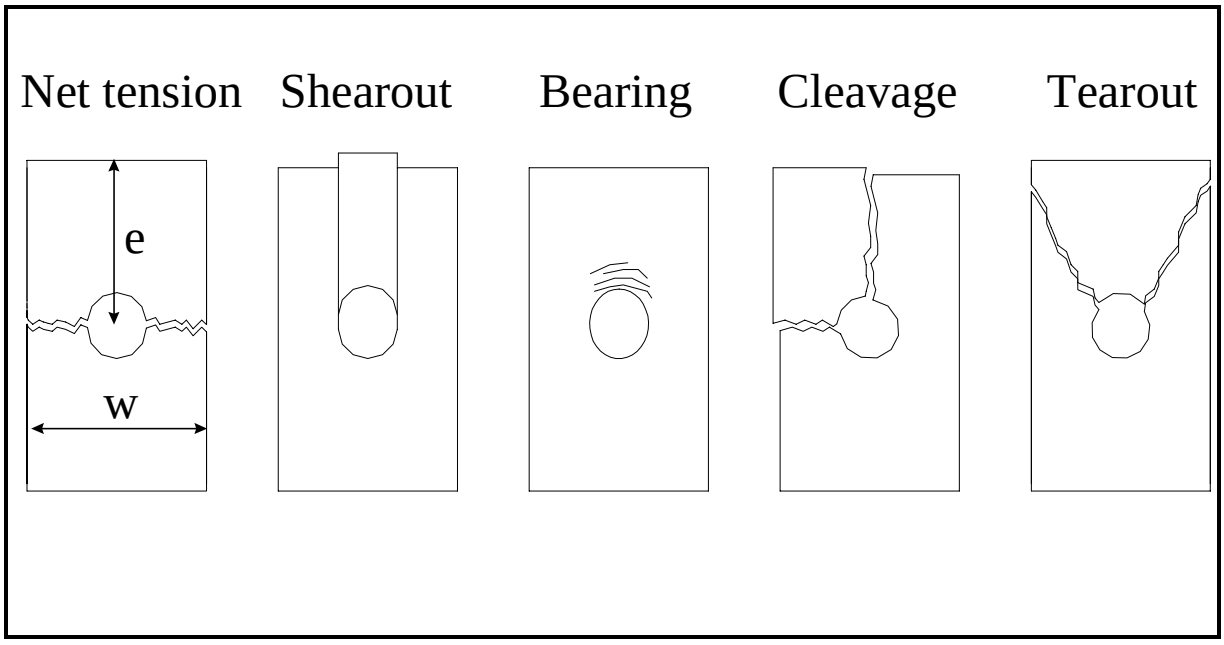

Fig. 1: Failure modes for shear loaded bolted joints

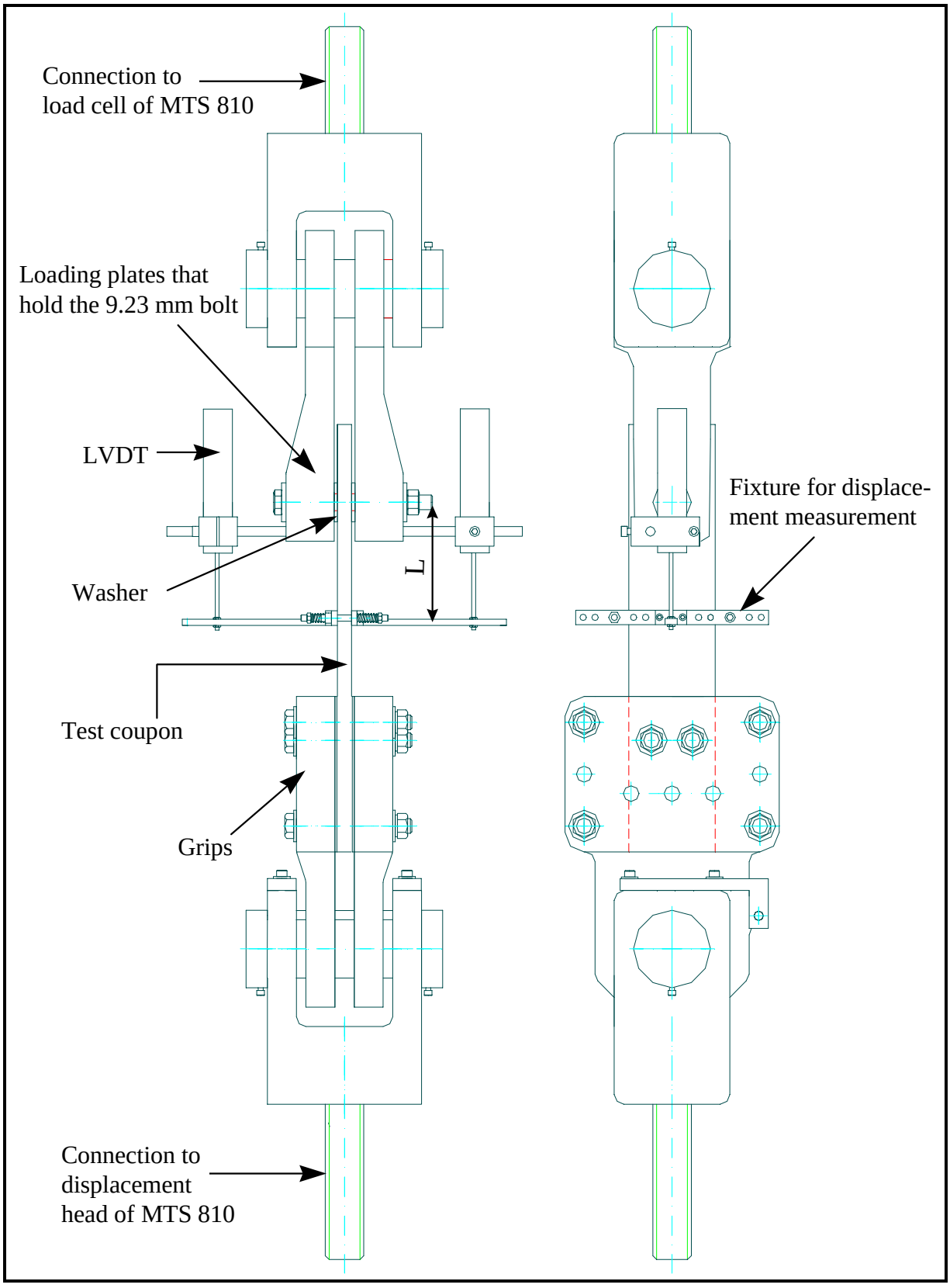

Fig. 2:Testing fixture for bolted joint tests

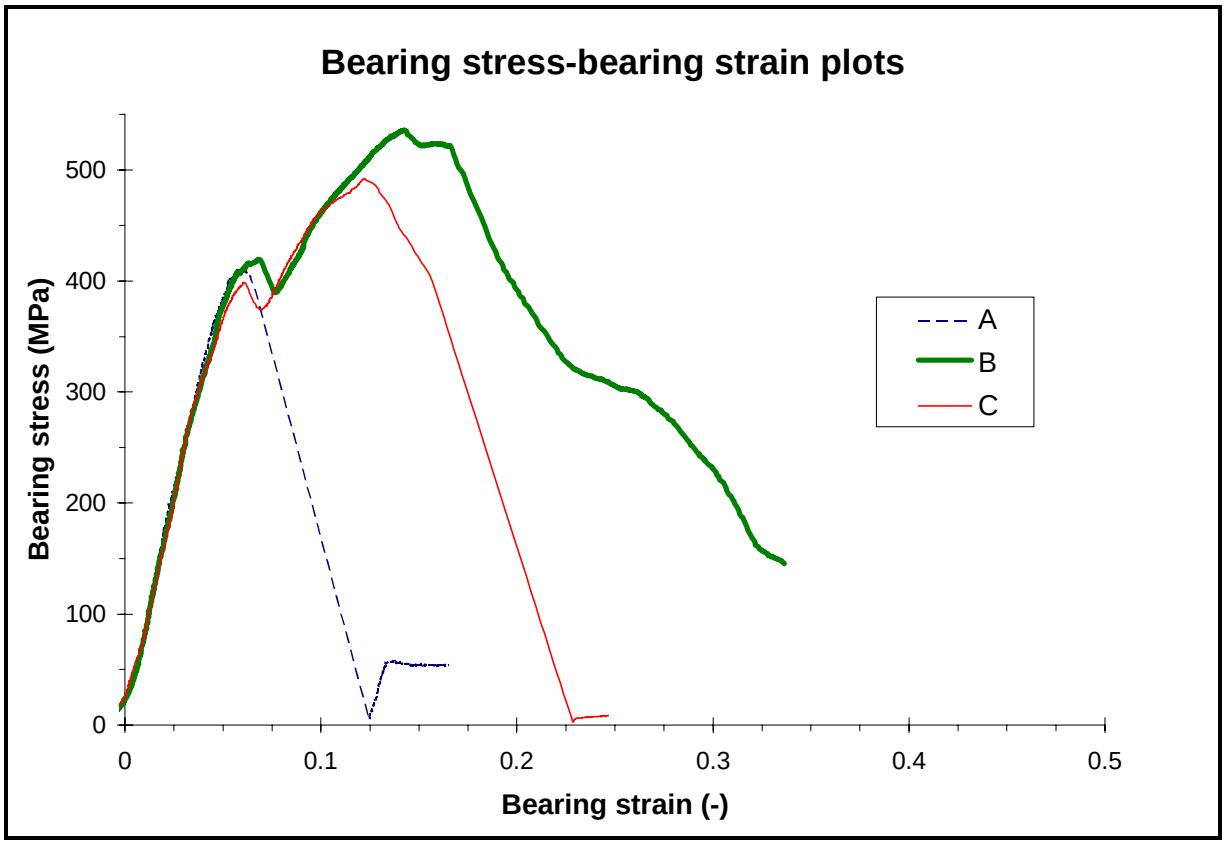

Fig. 3: Bearing stress - bearing strain curves for laminates A, B and C.

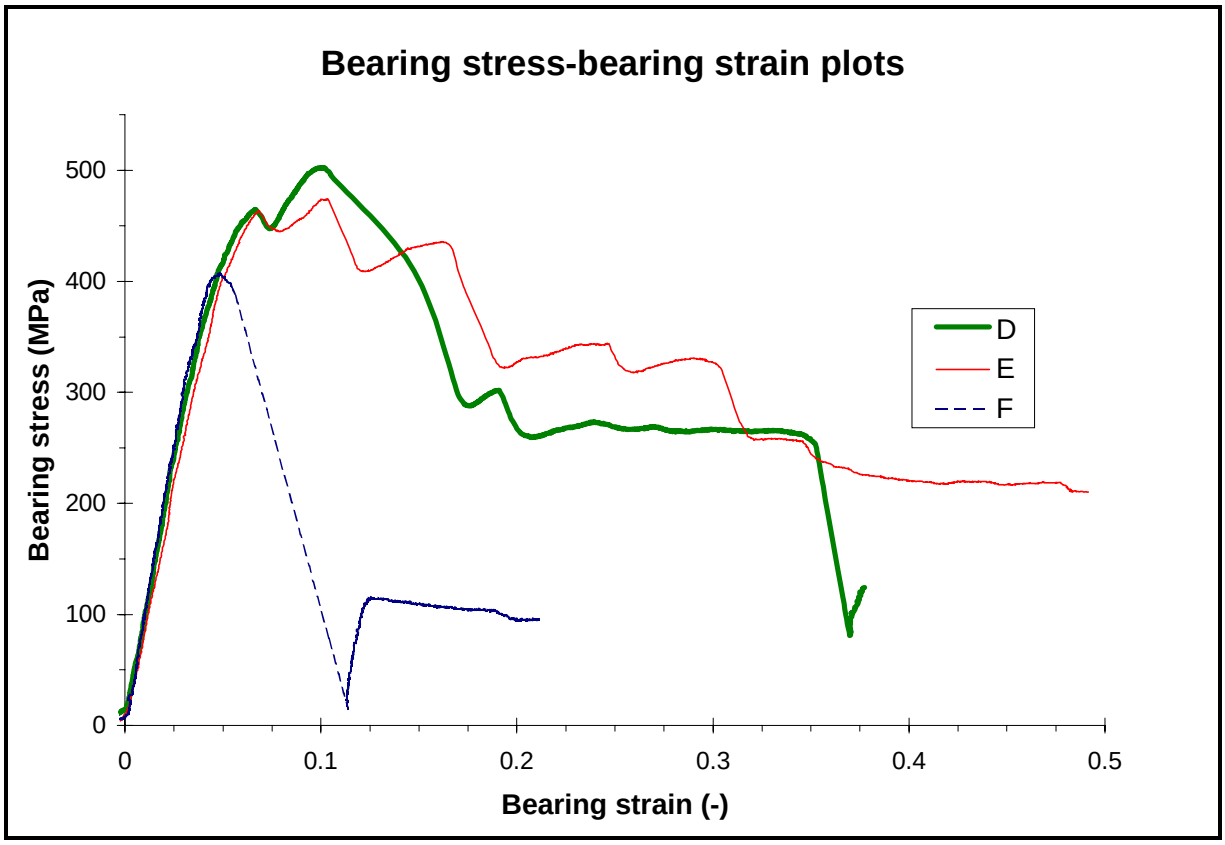

Fig. 4: Bearing stress - bearing strain curves for laminates D, E and F.

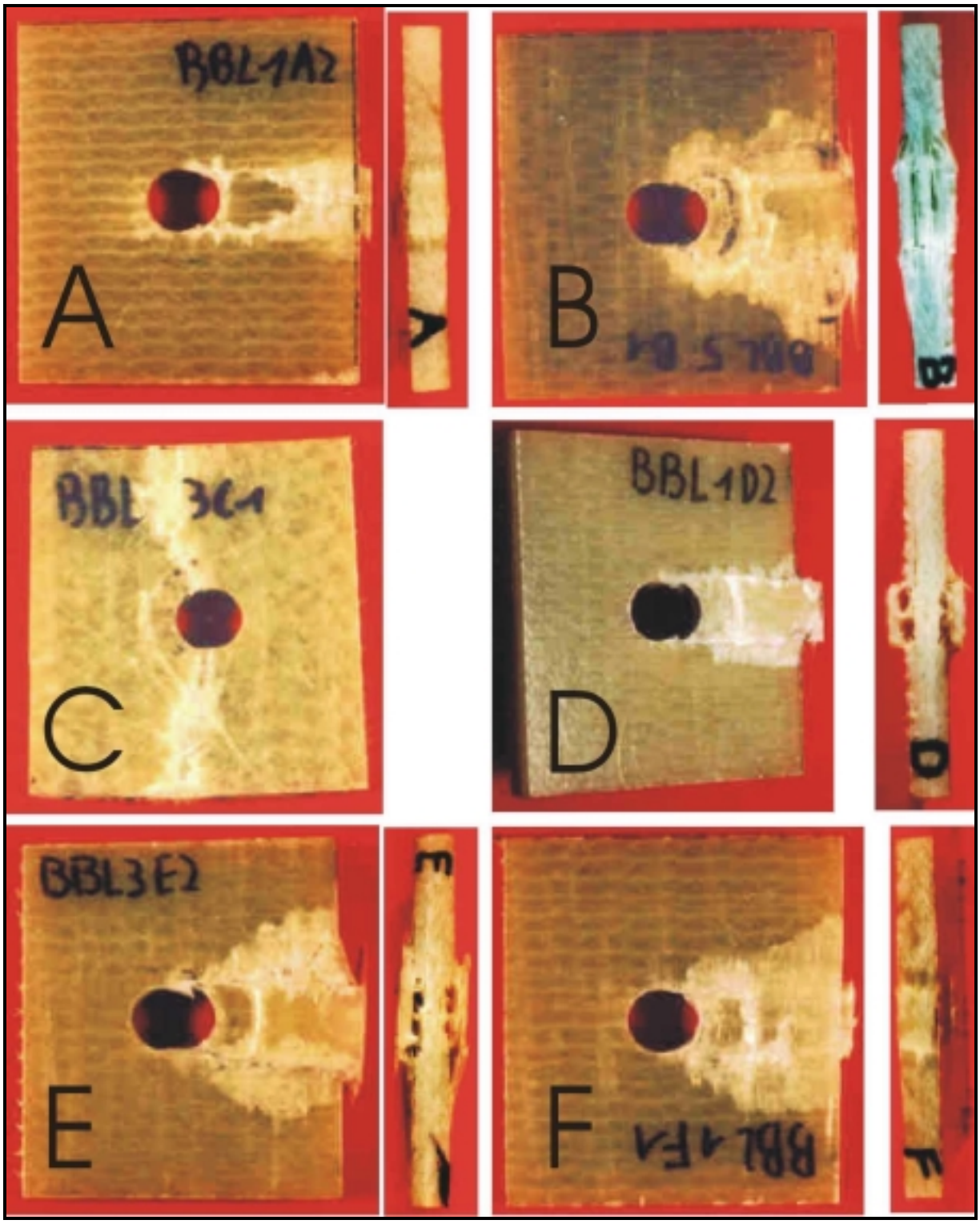

Fig. 5: Failure modes